HOSTED BY

ELSEVIER

Available online at www.sciencedirect.com

ScienceDirect

Soils and Foundations 60 (2020) 1570–1587

SOILS AND FOUNDATIONS

www.elsevier.com/locate/sandf

Technical Paper

An experimental study on the parameters affecting the cyclic lateral response of monopiles for offshore wind turbines in sand

Dennis Frick *, Martin Achmus

Institute for Geotechnical Engineering, Leibniz University Hannover, Germany

Received 8 January 2020; received in revised form 7 September 2020; accepted 13 October 2020
Available online 5 November 2020

Abstract

The design of monopile foundations for offshore wind turbine structures is dominated by requirements resulting from serviceability and fatigue limit state. To fulfil these criteria, the load deflection-behaviour and therefore long-term accumulations of permanent deflections and rotations of the monopile foundation due to cyclic occurring wind and wave loads have to be predicted. In this paper a brief overview on current design code practice as well as other proposed methods for the prediction of accumulated deflections or rotations is given. Further, the results of a systematic model test study dealing with the response of monopiles to lateral cyclic loading in medium dense sand at different cyclic load ratios, load eccentricities and pile embedment lengths are described and evaluated. The observations of the model test study are supplemented by results of a second test series involving the visualisation of displacement fields around laterally loaded piles by means of particle image velocimetry. Based on the findings and the results of previous experimental investigations, recommendations regarding the prediction of displacement accumulations for large diameter monopiles in sand are given.

Keywords: Monopiles; Offshore wind turbine foundations; Lateral cyclic loading; Pile deflection accumulation; 1g model tests; Particle image velocimetry

1. Introduction

Driven by the demand for renewable energies and the reduction of greenhouse gas emissions a rapid development in the planning and construction of new offshore wind farms is taking place for several years now. From a geotechnical point of view, new ground is constantly broken as the rated power of the offshore wind energy converters (OWECs), water depths of future wind farm sites and thus the size of the wind turbines itself as well as the associated towers and foundations transferring the arising loads to the seabed are constantly increasing. This makes the design of future foundation systems a demanding task. Available foundation solutions can be divided in pile foundations such as monopiles, jackets and tripods, gravity based foundations or suction buckets, whereby, up to now the monopile is the preferred foundation type for low to medium water depths. In European waters the monopile foundation has been used for approximately 66% of all newly erected OWECs in the year 2018. With respect to the total amount of installed offshore wind turbines in Europe, the monopile currently represents 81.9% of all substructures (Walsh, 2019). Its high popularity can be addressed to its relatively simple design, robustness in most soil conditions and suitability for mass production.

In practice and according to the current offshore guidelines the common design method for the prediction of the lateral response of monopiles is the p-y-method. It assumes the pile to be an elastic beam supported by soil medium, which is represented as a series of uncoupled springs acting normal to the beam element. The non-linear spring charac-

Peer review under responsibility of The Japanese Geotechnical Society.
* Corresponding author.
E-mail addresses: frick@igth.uni-hannover.de (D. Frick), Achmus@igth.uni-hannover.de (M. Achmus).

https://doi.org/10.1016/j.sandf.2020.10.004
0038-0806/

teristic curves (p-y curves) are describing the soil's bedding resistance p dependent on the lateral pile displacement y and are therefore decisive for an accurate and reliable design. Existing approaches for the determination of p-y curves, as those proposed in the API (2014) recommendations, are largely based on field tests on small-diameter (<1 m), long and therefore slender piles reported by Reese et al. (1974), Murchison and O'Neill (1984) and others. Even though application of these approaches for the dimensioning of oil and gas structures has shown sufficient accuracy, concern over the applicability to large diameter monopiles has been expressed. A series of theoretical considerations and numerical investigations reported in literature revealed several shortcomings of the conventional p-y expression stated in API (2014) when applied to large diameter piles. Therefore, in recent years various adopted methods have been proposed to improve the prediction of the monotonic monopile response using the p-y method (e.g. Sørensen, 2012; Kallehave et al., 2012; Thieken et al., 2015). Most recently, as an outcome of the joint industry Pile Soil Analysis project (PISA) a new design method for monotonic lateral and moment loading of monopiles has been introduced. The PISA design model is still based on the idealization of the pile as a beam supported by non-linear springs, but incorporates additional soil reaction components, e.g. shear tractions induced at the pile perimeter and a force as well as a moment reaction applied to the pile tip, to improve the model's performance. Development and calibration of the PISA method included results of 3D finite element modelling that had been calibrated against large scale field test data (Byrne et al., 2017; Byrne et al., 2019, amongst others). Given the significant improvements regarding the prediction of the monotonic load–displacement response of monopiles and the known deficits of different p-y expressions, latest offshore design codes such as DNV GL (2018) do not demand the use of a specific p-y method anymore. Instead, a recommendation is included demanding any design approach for piles with diameters of more than 1.0 m should be validated by means of other methods such as FE calculations.

Next to the load bearing behaviour of a monopile due to monotonic loading, another crucial aspect in the design of monopile foundations is the consideration of cyclic loads from the action of wind and waves. As these horizontal cyclic loads are in general large in proportion to the gravitational loads, they may lead to an accumulation of significant permanent displacements or rotations of a monopile and the overlying tower. To fulfil serviceability criteria (SLS) these deformations have to be predicted and limited for the complete design lifetime of the structure. The tilt tolerance and allowable permanent foundation rotation at soil surface are usually defined by the turbine manufacturer as they depend on the turbine type. As a typical limiting rotation of the pile head at soil surface the DNV GL (2018) suggests a value of 0.5° inclusive of a 0.25° constructional tolerance, which means the limit for the permanent allowable accumulated rotation due to cyclic loading to be 0.25°.

To account for the effect of cyclic loading in the design, the conventional p-y method approach proposed by the API (2014) is extended by an empirical calibration factor, which leads to a degradation in stiffness and ultimate soil resistance of 70% at seabed level, decreasing linearly with depth down to $z = 2.625 \cdot D$. Below this point the p-y curves for monotonic and cyclic loading are equal. Application of this procedure results in an overall softer foundation response and a reduced monopile capacity. Although this approach provides a pragmatic way of extending the static p-y method to cyclic loading, it does not account for the complex processes that are associated with cycling and that may in consequence lead to significant changes in foundation performance. As relatively large foundation stiffness is demanded in the dimensioning process of a monopile foundation to ensure a natural frequency of the complete system that is within the "soft-stiff" window, the API (2014) approach may lead to uneconomical foundation dimensions. Given the criticality of the SLS proof in the dimensioning process and the fact that the API (2014) calibration factor was empirically derived from field tests with less than 100 load cycles, this method is widely deemed as not being adequate for monopile foundations since neither the number of load cycles nor the cyclic load characteristics are considered. Hence, a large number of enhanced methods for the prediction of cyclic displacement accumulation and changes in foundation stiffness have been proposed.

In this paper a short literature review on some of these proposals dealing with the deflection accumulation due to cyclic horizontal loading is given. Further, the results of new small-scale monotonic and cyclic experiments are evaluated and discussed, whereby connection to other studies is drawn. Finally, additional results of a small scale test series involving particle image velocimetry are used to reveal processes occurring in the near field of a laterally loaded pile while cycling. In the end, all findings are used to make recommendations on how to deal with the deflection accumulation of a monopile subjected to lateral cyclic loading.

2. Literature review on pile behaviour under cyclic lateral loading

Due to before mentioned shortcomings of current methodology proposed by the offshore guidelines leading to uncertainties in the design or on the other hand uneconomical over-dimensioning when applied to large diameter monopile foundations, various researchers made efforts to investigate the parameters influencing cyclic pile behaviour and develop more precise predictive models. As full scale test data especially for rigid piles is rare in literature, most publications relate to cyclic model scale experiments or numerical results. In most cases numerical approaches

are still at development stage or need further validation. For this reason, the majority of reported studies are based on small scale experiments either at 1 g or in the centrifuge. The results of these are mostly presented along with best-fit curves or formulations as a means for practical and cost-effective methods to assess accumulated pile displacements or rotations. Anyway, it has to be kept in mind, these approaches vary in terms of the underlying pile behaviour (rigid or flexible), number of applied load cycles and cyclic loading characteristics (one-way or two-way loading, maximum cyclic load). The before mentioned pile behaviour or relative pile-soil stiffness respectively is an important indicator for the general behaviour of a pile. While rigid piles are short compared to their diameter, they undergo rigid body rotation in the soil instead of bending, which means the shear strength of the soil governs the design and the soil fails before the pile. On the other hand, long and slender piles undergo a more flexible behaviour with bending and typically fail through formation of a plastic hinge. Due to cyclic loading, for a rigid pile higher degradation may be expected compared to flexible piles because soil deformation and degradation of soil stiffness occur over the entire length of the pile. For the characterisation of the relative pile-soil stiffness, different methods such as the non-dimensional relative stiffness ratio proposed by Poulos and Hull (1989) can be found in literature. While early large scale tests on piles in sand were carried out on long and flexible piles with a limited number of load cycles not being representative for offshore monopiles, more recent model test campaigns considered dimensions and loading conditions comparable to typical monopile foundations (e.g. rigid pile behaviour and higher number of load cycles). Due to the complexity of the mechanisms driving displacement accumulation and inherent differences in reported tests, disagreements in results of different studies are to be expected. Therefore, careful examination of the assumptions and the applicability of each proposed method is required.

Based on 34 cyclic full-scale tests on laterally loaded piles with different sizes which mostly exhibited flexible behaviour, Long and Vanneste (1994) studied the effect of cyclic load ratio (M_{min}/M_{max}), installation method and the effect of soil density on the modulus of subgrade reaction. To account for the effects of cyclic lateral loading, they proposed degrading factors as shown in Eq. (1) and Eq. (2) for calculating the soil resistance p and soil deflection y which can be used to produce adjusted non-linear p-y curves.

$$p_N = p_1 \cdot N^{-0.4t} \tag{1}$$

$$y_N = y_1 \cdot N^{0.6t} \tag{2}$$

Here N is the number of load cycles and t is the degrading parameter that is defined by Eq. (3):

$$t = 0.17 \cdot F_L \cdot F_I \cdot F_D \tag{3}$$

The factor F_L herein depends on the cyclic load ratio and was recommended to be 1.0 for one-way loading ($M_{min}/M_{max} = 0$) and 0.2 for two-way loading ($M_{min}/M_{max} = -1$). Further F_I is a factor related to the installation method and ranges from 0.9 to 1.4, while F_D depends on the soil density and takes values between 0.8 and 1.1. From the above it may be concluded that the governing degradation parameter is the load ratio where highest accumulation results from one-way loading. With respect to the dimensioning of monopile foundations it is important to note that the underlying tests of this method involved a maximum of 50 load cycles on mainly flexible piles, which is significantly different from the conditions that are experienced by typical offshore monopiles.

Using a similar approach, Lin and Liao (1999) derived a degradation parameter to calculate cyclic strains ε from 20 full-scale tests reported in literature and validated them against 6 additional pile tests. The underlying tests included both rigid and flexible piles, most of which exhibited a rather flexible behaviour. Comparable to Long and Vanneste (1994) they found the degradation parameter to be dependent on the cyclic load ratio, installation method and soil density. For the calculation of cyclic strains Lin and Liao (1999) suggest the logarithmic approach shown in Eq. (4) with the degradation parameter t given in Eq. (5).

$$\varepsilon_N = \varepsilon_1 \cdot (1 + t \cdot \ln(N)) \tag{4}$$

$$t = 0.032 \cdot L \cdot \sqrt[5]{\frac{\eta_h}{E_p I_p}} \cdot \beta \cdot \xi \cdot \varphi \tag{5}$$

where L is the pile embedment length, E_pI_p is the pile bending stiffness, N is the number of load cycles, η_h is the modulus of subgrade reaction, β depends on the soil density and ranges from 1.0 for dense sand to 1.3 for loose sand, ξ describes the pile installation method (0.3 for vibrated to 1.8 for backfilled) and ϕ considers the effect of cyclic load ratio with recommended values between 1.0 for one-way loading ($M_{min}/M_{max} = 0$) and 0.09 for two-way loading ($M_{min}/M_{max} = -1$). Also from this approach, which is based on tests with a maximum of 100 load cycles, highest accumulation can be found to result from one-way loading.

An extensive experimental study specifically focused on the pile rotation accumulation of rigid and large diameter monopiles was conducted by LeBlanc et al. (2010). The study was based on a series of 1 g model tests, where horizontal loads H were applied to a scaled monopile ($L/D = 4.5$) with a load eccentricity of $h = 1.2 \cdot L$ (distance of load application point to soil surface) and load cycle numbers (N) of at least 7000 up to 65000. The model pile was embedded in dry silica sand with relative density D_r of either 4% or 38% and an embedment length of $L = 360$ mm. To clearly characterise the applied cyclic loads, LeBlanc et al. (2010) introduced two load parameters, namely cyclic load magnitude ζ_b and cyclic load ratio ζ_c as given in Eq. (6) and Eq. (7).

$$\zeta_b = \frac{M_{max}}{M_{ult}} = \frac{H_{max} \cdot e}{H_{ult} \cdot e} \tag{6}$$

$$\zeta_c = \frac{M_{min}}{M_{max}} = \frac{H_{min} \cdot e}{H_{max} \cdot e} \quad (7)$$

Here, M_{ult} refers to the static moment capacity of the pile derived from a monotonic load-rotation curve by application of a specific pile failure criterion ($\theta = 4°$). M_{min} and M_{max} are the minimum and maximum moments resulting from cycling within a load cycle. Corresponding horizontal forces H follow from H = M/h. On basis of the conducted tests LeBlanc et al. (2010) proposed a power function according to Eq. (8) to predict permanent increases in pile head rotation $\Delta\theta$ with load cycle number N:

$$\Delta\theta(N) = \theta_1 \cdot T_b(\zeta_b, D_r) \cdot T_c(\zeta_c) \cdot N^{\alpha} \quad (8)$$

For the accumulation parameter they recommend an empirically derived value of $\alpha \approx 0.31$. The factors T_b and T_c were found to be dependent on load characteristics as well as soil relative density and have been defined in terms of different functions as depicted in Fig. 1. T_b can be seen to linearly increase with load magnitude ζ_b and to vary with soil relative density. On the other hand, the T_c-function is not affected by soil relative density and indicates the influence of cyclic load ratio ζ_c on the pile rotation accumulation. Following this approach, it emerges that an asymmetric two-way load with a cyclic load ratio of $\zeta_c = -0.6$ and a given load magnitude will result in 4 times higher accumulated rotations compared to a one-way load with complete unloading in each cycle, i.e. $\zeta_c = 0$.

Another study involving centrifuge model tests on almost rigid piles in dry and saturated sand has been reported by Klinkvort and Hededal (2013). In their tests, they applied up to 500 load cycles with a load eccentricity of h = 2.5·L and load magnitudes ζ_b ranging from 0.08 to 0.36. Similar to LeBlanc et al. (2010) they found the maximum accumulation rate to be independent from load magnitude and to result from cyclic loads with $\zeta_c = -0.4$. Despite these basically comparable results, Klinkvort and Hededal (2013) derived a maximum T_c-value that was only slightly greater than 1 and therefore significantly smaller than the one found by LeBlanc et al. (2010) with a value of approximately 4.

Truong and Lehane (2015) conducted a series of centrifuge tests on model monopiles as well. In these tests, the dry sand samples had a relative density of 40% and loads have been applied with a lever arm of h = 0.14·L. The chosen load magnitudes ζ_b were rather high, having values of more than 1, which results from the fact that pile capacity was specified at a pile head displacement of only 0.1·D. From the tests a maximum pile head accumulation rate has been obtained for $\zeta_c = -0.37$. Since Truong and Lehane (2015) used a power function as shown in Eq. (9) to directly fit pile head displacements (and not accumulations), no increase factors with respect to cyclic one-way loading, i.e. a T_c-function, has been reported. In Eq. (9) $y_{head,N}$ is the pile head displacement after application of N load cycles while $y_{head,N=1}$ is the pile head displacement after the first load cycle or the displacement due to a static load for a given load level respectively. α_y is an accumulation parameter for the pile head displacement (not rotation).

$$y_{head,N} = y_{head,N=1} \cdot N^{\alpha_y} \quad (9)$$

To systematically study the influence of different geometry and boundary conditions on the pile deflection accumulation, Albiker et al. (2017) executed 1-g model tests on four different pile-soil systems varying relative pile-soil stiffness (flexible or rigid), relative soil density (D_r = 40% or D_r = 60%) and load eccentricity (h = 0.71·L or h = 0.36·L). All test series involved 2500 load cycles with different cyclic load ratios ζ_c at a constant load magnitude of $\zeta_b = 0.3$, whereby pile capacity has been defined by a pile displacement criterion. For the almost rigid pile-soil systems T_c-functions similar to that proposed by LeBlanc et al. (2010) have been found, having maximum T_c-values between 1.35 and 1.72 for an unbalanced two-way loading ($\zeta_c = -0.33$). Soil relative density influenced neither the shape nor the maximum of the function significantly. On the opposite, a higher load eccentricity resulted in higher $T_{c,max}$-values.

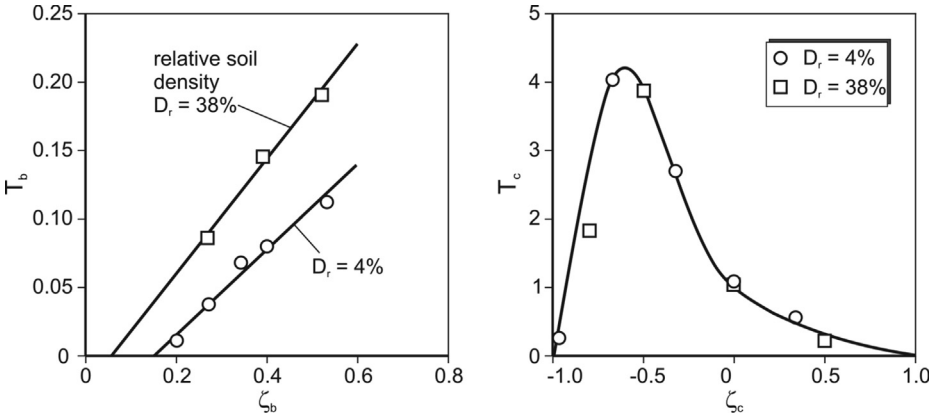

Fig. 1. T_b- and T_c-functions proposed by LeBlanc et al. (2010).

A recent study of Truong et al. (2019) involved 17 centrifuge pile tests with different relative sand densities (D_r = 51% to D_r = 95%), pile slenderness ratios (L/D = 6 to L/D = 11.4) and load magnitudes (ζ_b = 0.45 to ζ_b = 1.05). Pile capacity has been defined by a pile rotation of 0.5° at sand surface. Also load eccentricity varied in the range of h/D = 2 to h/D = 3 and cyclic loads have been applied with different cyclic load ratios. Based on the self-conducted test series and the results of Klinkvort and Hededal (2013), Li et al. (2015) as well as Rosquoët et al. (2007), Truong et al. (2019) also proposed Eq. (9) to predict pile head displacements after N load cycles. In order to account for different relative sand densities ($D_r > 0.5$) and cyclic load ratios Eq. (10) is introduced to describe an upper-bound curve for the accumulation parameter α_y.

$$\alpha_y = (0.3 \pm 0.22 \cdot D_r) \cdot \left[1.2 \cdot \left(1 - \zeta_c{}^2\right) \cdot (1 - 0.3 \cdot \zeta_c)\right] \quad (10)$$

According to this approach, maximum accumulations result from cyclic load ratios of about $\zeta_c = -0.5$ and lower soil densities. Further Truong et al. (2019) found that α_y is largely independent from cyclic load magnitude ζ_b and the eccentricity of applied loads (e/D), though $y_{head,N=1}$ in Eq. (9) of course depends on these parameters.

Considering the above and the in part divergent findings reported, it is evident that there is no clear conclusion in literature on the parameters affecting the cyclic displacement accumulation and to what extent they do so. However, there is consensus that highest accumulation rates for rigid piles (like monopiles) result from asymmetrical two-way loads. As a numerical study and assessment on 15 operating wind turbines in European waters by Jalbi et al. (2019) has shown the load ratio to vary widely ranging from one-way loading under normal operational conditions to two-way loading for extreme wind and wave loading scenarios (especially in deep waters), it becomes obvious that there is a need for further clarification. The systematic investigation presented in the paper at hand is intended to contribute to the understanding of the mechanisms on which the pile displacement accumulation depends and the influencing factors.

3. Small-scale model tests

3.1. Test program

The experimental test program was designed to study and identify the parameters affecting the pile displacement accumulation of a rigid monopile due to lateral cyclic loading. In particular, the influence of load eccentricity or the ratio of horizontal force to overturning moment respectively, pile embedment length, number of load cycles and load magnitude on the shape of the loading type function $T_c(\zeta_c)$ and the accumulation parameter α as proposed by LeBlanc et al. (2010) should be evaluated. Further, the magnitude of influence of the respective parameters shall be investigated.

The complete test program comprised more than 96 tests including both, monotonic and cyclic loading, on two different pile-soil systems in dry sand having a relative density D_r of approximately 40% (medium dense). The model pile used in the tests was an aluminium pipe having an outer diameter of D = 50 mm and a wall thickness of t = 3.2 mm. Two different embedment lengths of L = 400 mm (L/D = 8) and L = 300 mm (L/D = 6) are considered by which the pile-soil system 1 (L/D = 8, D_r = 0.4) and pile-soil system 2 (L/D = 6, D_r = 0.4) are defined. Applying the non-dimensional stiffness ratio suggested by Poulos and Hull (1989), both pile-soil systems can be classified to behave almost rigid, similar to a true scale monopile. The ratio of load eccentricity h to embedment length L has been varied in the range of h/L = 0.6 to h/L = 1.0 for system 1 and h/L = 0.8 to h/L = 1.2 for system 2.

For the purpose of better comparability between different pile-soil systems and load eccentricity configurations, all applied loads have been defined by means of load magnitude ratio ζ_b and cyclic load ratio ζ_c as already introduced in Eq. (6) and Eq. (7). The value of the load magnitude ratio was set to $\zeta_b = 0.35$ in all tests except test series 4 (c) (see Table 1). Corresponding pile capacities H_{ult} for each configuration have been derived from displacement controlled monotonic load tests ($\zeta_c = 1$) by application of a pile failure criterion (see below). To evaluate the displacement accumulation behaviour due to arbitrary cyclic one- and two-way loading conditions, the cyclic load ratio was assigned to values of $\zeta_c = -0.75/-0.50/-0.25/0.00/+0.25$ for all test series, each involving a minimum of 2500 sinusoidal load cycles at a constant load frequency of 0.1 Hz. To prove redundancy, each configuration has at least been tested twice. Table 1 provides an overview of the test schedule along with the related system parameters and load characteristics.

3.2. Test equipment

The small scale model tests were performed using a new designed testing rig, consisting of a cylindrical sand container, a model monopile, an actuator and several sensors (see Fig. 2). The sand container has an inner diameter of 600 mm and a depth of 750 mm. As the model monopile has an outer diameter of D = 50 mm, the ratio of the inner diameter of the sand container and the pile diameter is 12. According to numerical simulations of Albiker et al. (2017), who modelled a sand container with diameter of 600 mm as well as a much larger container and a laterally loaded pile with diameter of D = 60 mm in sand with relative density of D_r = 0.4, the dimensions of the utilized sand container are sufficient so that boundary effects are expected to be negligible. For the application of monotonic and cyclic one- and two-way loads to the model monopile an electromechanical actuator with a maximum stroke range of 400 mm and a maximum capacity of 2 kN was

Table 1
Test program.

Pile-soil system description						Load description		
Test series [#]	System [#]	D [mm]	L/D [–]	e/L [–]	D_r [–]	ζ_b [–]	ζ_c [–]	N [–]
1	1	50	8	0.6	0.4	0.35	−0.75/−0.50/0.25/0.00/0.25/1.00	2500
2	1	50	8	0.8	0.4	0.35	−0.75/−0.50/0.25/0.00/0.25/1.00	2500
3	1	50	8	1.0	0.4	0.35	−0.75/−0.50/0.25/0.00/0.25/1.00	2500
4 (a)	2	50	6	0.8	0.4	0.35	−0.75/−0.50/0.25/0.00/0.25/1.00	2500
4 (b)	2	50	6	0.8	0.4	0.35	−0.75/−0.50/0.25/0.00/0.25/1.00	10,000
4 (c)	2	50	6	0.8	0.4	0.20	−0.75/−0.50/0.25/0.00/0.25/1.00	2500
5	2	50	6	1.0	0.4	0.35	−0.75/−0.50/0.25/0.00/0.25/1.00	2500
6	2	50	6	1.2	0.4	0.35	−0.75/−0.50/0.25/0.00/0.25/1.00	2500

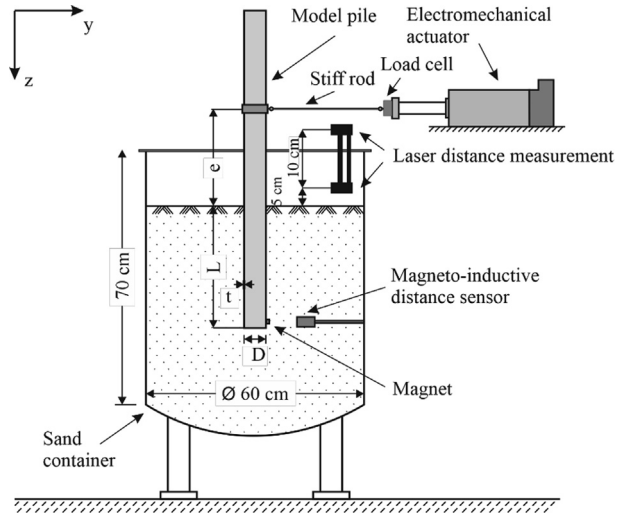

Fig. 2. Experimental set-up.

used. The actuator is installed on a stiff frame that is attached to the sand container and adjustable in height to enable load application with different load eccentricities. The connection between actuator and model pile was realized by a rigid rod with hinged connections on both sides to allow free rotation of the pile around the x-axes (see Fig. 2) during load application. The measurement equipment of the testing arrangement includes a high precision load cell with a capacity of 1 kN which is attached to the actuator, two laser distance transducers (LDTs/product: Allsens AM300) set perpendicular to the pile at heights of 50 mm and 150 mm above sand surface and a magneto-inductive displacement transducer (product: Micro Epsilon MDS-45-M12-CA) that can be arranged within the sand container at height of the pile toe for the contactless measurement of pile tip movements. The two LDT measurements allow the calculation of lateral pile head displacements y_{head} at the sand surface or the determination of pile rotations θ. Physical quantities measured in y-direction, such as displacements or forces imposed by pulling with the actuator, are positive.

3.3. Soil properties and sand sample preparation

The F34 sand used in the small-scale tests is a fine to medium grained silica sand having a mean effective particle size of $d_{50} = 0.18$ mm and a uniformity coefficient of $C_u = 1.90$. Further characteristic sand parameters are summarized in Table 2. The grain size distribution is provided in Fig. 3. A more detailed description of the sand and results of static as well as cyclic consolidated-drained triaxial tests can be found in Albiker (2016).

The sand sample preparation was done by air pluviation. In a preliminary investigation it could be shown that this technique provides homogeneous and reproducible sand conditions in a normally consolidated state. To avoid influences of the pile installation (complex stress-fields and local density changes) on the test results and still be able to mobilize a pile base shear force, the sand container was first filled with sand to a height of about 5 cm above the later position of the pile toe. Then the open ended model pile was slightly pushed into the sand and fixed in position before the sand sample preparation was completed around the pre-installed pile. In the present study a relative density D_r of approximately 0.4 corresponding to a soil dry unit weight of $\gamma(D_r = 0.4) = 15.0$ kN/m^3 was chosen.

3.4. Scaling considerations

The basis of this study is a set of monotonic and cyclic laboratory experiments on stiff model monopiles in sand conducted at 1 g. The transfer of such small-scale test results to a prototype system is a demanding task and scaling laws have to be considered. Even though the results of this study are initially intended to gain insights into the qualitative influences of various parameters on the displacement accumulation, some considerations were made with regard to scaling issues. Taking into account the principle variables governing the lateral pile behaviour, pile displacements y can generally be expressed by a set of

Table 2
F34 silica sand properties.

Description	Parameter	Unit	Value
Mean grain size	d_{50}	[mm]	0.18
Uniformity coefficient	C_u	[–]	1.90
Coefficient of curvature	C_c	[–]	1.02
Minimum void ratio	e_{min}	[–]	0.585
Maximum void ratio	e_{max}	[–]	0.887
Grain density	ρ_s	[g/cm^3]	2.65

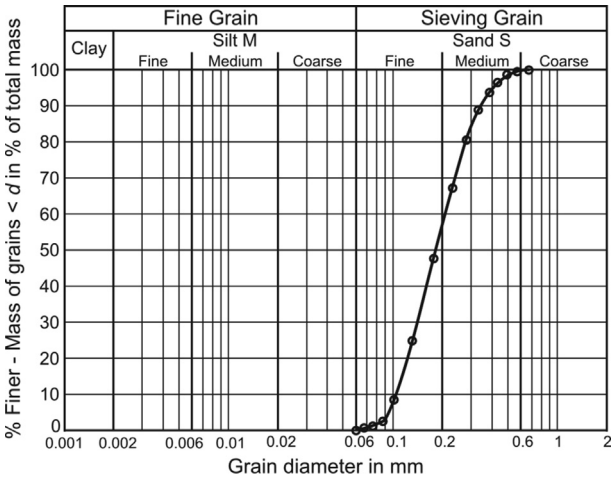

Fig. 3. F34 silica sand grain size distribution.

non-dimensional terms as given in Eq. (11) using Buckingham's theorem (Peralta and Achmus, 2010).

$$\frac{y_N}{L} = f\left(\frac{L}{D}, \frac{h}{L}, \frac{H}{\gamma L^3}, \frac{E_p I_p}{\gamma L^5}, e, N\right) \tag{11}$$

Anyway, due to the nature of small-scale 1 g model tests, the isotropic stress level dominating the frictional behaviour of the sand is low and the volume change behaviour of the soil differs from that in true scale. Dilatancy in response to shearing is generally overestimated and this is accompanied by higher friction angles. Furthermore, also soil stiffness is stress dependent and tends to be underestimated in 1 g experiments when compared to full scale. A possible solution to avoid the stress dependent increase of the dilatancy for small overburden pressures in 1 g testing is a reduction of the soil relative density as proposed by LeBlanc et al. (2010). Nevertheless, this will induce other scaling issues, such as a further reduction in soil stiffness, and has not been done in the tests described in the present study. As an investigation regarding the effect of stress-level on the response of a model monopile to cyclic lateral loading in sand by Richards et al. (2020) shows, the results of 1 g model tests can nevertheless contribute to the understanding of the monopile behaviour. According to Richards et al. (2020), who conducted a series of monotonic as well as cyclic small scale experiments either at 1 g, 9 g and 80 g - always using the same experimental set-up to isolate stress-level effects - it could be shown that the cyclic responses are qualitatively similar across the stress-levels, even though quantitative differences have been observed. For the accumulation parameter α (see Eq. (8)) they found a logarithmic decrease with stress level, which suggests the exponent α at full scale to be around half of the value obtained in 1 g tests. Further, no stress-dependency of the power law coefficient T ($T_b(\zeta_b,D_r)\cdot T_c(\zeta_c)$) in Eq. (8) describing only relative increases of deformations, i.e. the ratio of displacements due to monotonic and cyclic loading, was found. Based on these findings, the evaluation of the test results with respect to the loading type function $T_c(\zeta_c)$ proposed to LeBlanc et al. (2010) seems reasonable. However, results regarding the exponent α should be considered with caution against the background mentioned above.

Another aspect in model testing is the scaling of the sand grain diameter. To achieve better comparability with true scale tests, also sand particles should be scaled. A problem arises from the fact that this would change the nature and basic behaviour of the material. Nevertheless, for the chosen F34 silica sand and the model pile having a diameter of D = 50 mm a ratio of pile diameter D to mean grain diameter d_{50} of approximately 278 applies. According to literature, no scaling of sand particles is needed if a minimum ratio is kept. Typical reported values for D/d_{50} are ranging from 50 to 88 (Hoadley et al., 1981; Klinkvort, 2012). As D/d_{50} for the present tests is much higher than the proposed minimum values, no scaling of the sand grain diameter has been done.

Considering the before mentioned aspects, Eq. (11) yields that if geometric similarity is given, and load magnitude as well as relative system stiffness (flexible or rigid pile behaviour) are comparable, the same relative development of pile displacement or rotation accumulations can be expected for model and prototype scale (with exception of the accumulation parameter α). Thus, it seems justified to assume that $T_c(\zeta_c)$-functions derived from model tests can be transferred to true scale monopiles. Anyway, this assumption has to be further validated by means of either centrifuge or large-scale field tests.

3.5. Monotonic pile test results and evaluation

Monotonic load tests have been conducted in order to determine the respective pile capacity H_{ult} for both pile-soil systems and all investigated load eccentricities h. The pile capacity H_{ult} in ultimate limit state (ULS) for a given configuration provides a reference value for the cyclic load magnitude ζ_b (Eq. (6)) and therefore defines the maximum lateral load H_{max} in the corresponding cyclic tests. Fig. 4 presents the variations of normalised monotonic lateral load H with pile head displacement y_{head} at soil surface for pile soil-system 1 (left) and pile-soil system 2 (right), each with three different load eccentricities (h/L). The pile head displacements calculated from the two LDT measurements are depicted as solid lines. To prove repeatability of the sand sample preparation, each combination of pile-soil system and normalised load eccentricity (h/L) has at least been tested twice. As some scattering could be observed in the results for pile-soil system 2 with a load eccentricity of h/L = 1.2, this test has been done even four times.

From Fig. 4 it is evident, that total pile capacity has not been reached in the tests despite very large pile deflections. A distinct point of failure defined by a load–displacement curve approaching a horizontal tangent has not been measured. This behaviour is quite typical for laterally loaded piles as total failure of a rigid pile is associated with extensive deformations required for full plastification and

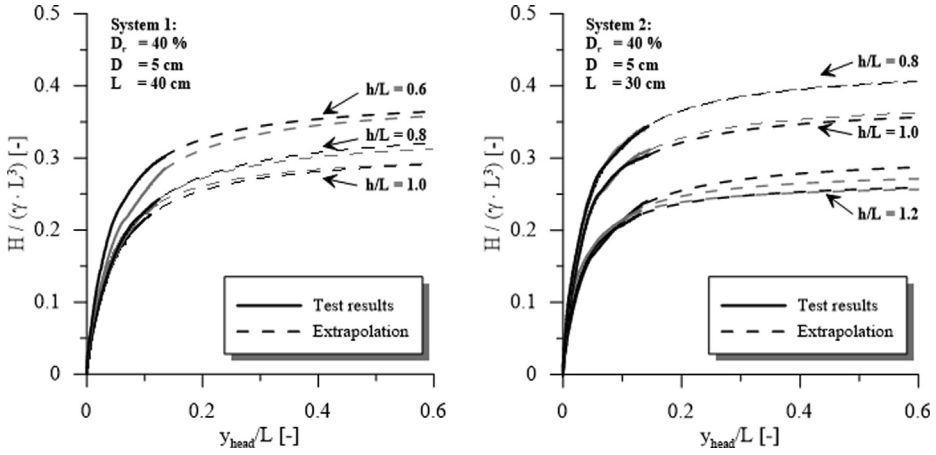

Fig. 4. Monotonic lateral pile test results.

mobilisation of the bedding material. Thus, pile capacity has to be defined in terms of another criterion. A problem arises from the fact that no general criterion for the definition of the pile capacity or pile failure exists. In literature a large number of different criteria related to a certain pile rotation or pile head displacement can be found (see Table 3). Also design standards do not provide guidance on a suitable definition.

As before mentioned criteria do not inevitably represent the total failure of a laterally loaded pile, the criterion or rather method of Manoliu et al. (1985) has been adopted in this study. The method assumes that load–displacement can be described by a hyperbolic function, which allows the determination of H_{ult} by extrapolation of measured test data. Extrapolation curves derived by application of this approach are depicted in Fig. 4 (dashed lines). Due to some slight scattering in the results, mean values for the pile capacity have further been used for each test configuration. Comparative calculations using the p-y method have been carried out to verify the plausibility of the extrapolation results. Fig. 5 provides a comparison of the pile capacities derived by p-y method calculations following the approach of Thieken et al. (2015) and extrapolation according to Manoliu et al. (1985). A comparative list of the results and the lateral soil parameters used for the p-y method calculation can be found in Table 4. It should be noted that the internal angle of friction ϕ' was set at 41° despite the medium relative density of the sand, which is due to the low stress conditions in 1 g-testing.

As it can be seen, in most cases the results derived by both methods are in good agreement. Accordingly, the method of Manoliu et al. (1985) seems to yield reasonable results that clearly define ultimate pile capacity H_{ult} for each configuration. For the present study, the results derived by Manoliu et al. (1985) depicted in Table 4 columns 3 and 5 were used as reference for the definition of load characteristics ζ_b and ζ_c for the cyclic tests.

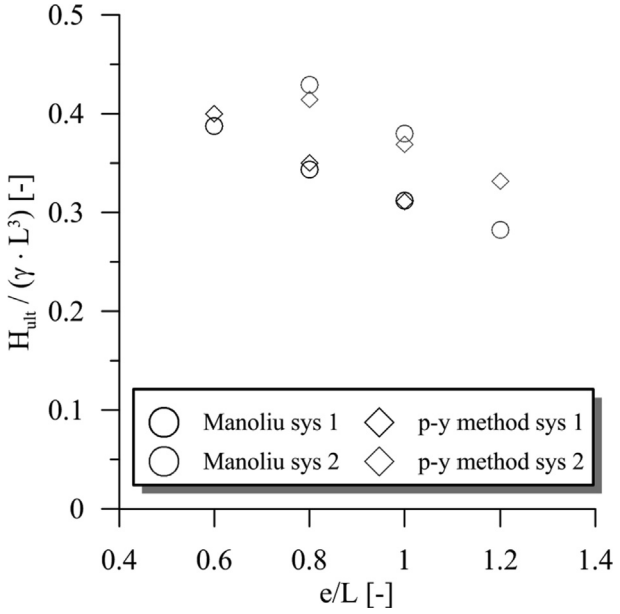

Fig. 5. Comparison of calculated and extrapolated pile capacities.

When comparing results to literature, it has to be kept in mind that ζ_b-values reported in other studies are not directly comparable as they depend on the chosen criterion for the definition of the pile capacity H_{ult}. In order to interpret the cyclic test results better and allow comparison to other studies, the monotonic tests have also been evaluated using alternative pile failure criteria. Table 5 shows the

Table 3
Examples for ULS failure criteria for laterally loaded piles.

Author	LeBlanc et al. (2010)	Peralta and Achmus (2010)	Truong and Lehane (2015)	Arshad and O'Kelly (2017)
Failure criterion	4° rotation	Pile head deflection 0.1·L	Pile head deflection 0.1·D	1.5° rotation

Table 4
Pile failure loads determined by test result extrapolation and p-y method calculation.

System	e/L	$H_{ult}/(\gamma \cdot L^3)$ [–]		H_{ult} [N]	
[#]	[–]	Extrapolation	p-y method*	Extrapolation	p-y method*
1	0.6	0.3875	0.4005	372.0	384.5
	0.8	0.3438	0.3505	330.0	336.5
	1.0	0.3122	0.3115	299.7	299.0
2	0.8	0.4296	0.4148	174.0	168.0
	1.0	0.3802	0.3691	154.0	149.5
	1.2	0.2825	0.3321	114.4	134.5

* p-y approach after Thieken et al. (2015) with $\varphi' = 41°$ and $\gamma' = 15$ kN/m^3.

chosen maximum cyclic loads H_{max} defined by the cyclic load magnitude $\zeta_b = 0.35$ and the method of Manoliu et al. (1985) as well as cyclic load magnitudes resulting from other typical pile capacity criteria for the given maximum cyclic loads. Despite significant differences and the relatively large loads due to the chosen pile failure criterion, the loading type function $T_c(\zeta_c)$ describing the pile deflection accumulation for a given pile-soil system, which is in the focus of this study, should - according to LeBlanc et al. (2010) - be independent of cyclic load magnitude ζ_b.

3.6. Cyclic pile test results and evaluation

The cyclic test results shall be used to derive loading type functions $T_c(\zeta_c)$ describing the pile head displacement accumulation $\Delta y_{head,N}/y_{head,N=1}$ in dependency on the cyclic load ratio ζ_c. In a first step, all cyclic tests with a cyclic load ratio of $\zeta_c = 0$ (one-way loading) have been investigated, as this type of loading represents the reference case for the loading type function ($T_c(\zeta_c) = 1$). In Fig. 6(a) the variation of measured maximum pile head displacements $y_{head,N}$ with load cycle number N is presented in a double logarithmic scale for both pile-soil systems and all test series according to Table 1. All measured curves are following a linear course, whereby the slopes of the variations for pile-soil system 1 (black lines) and pile-soil system 2 (grey lines) are slightly different, indicating an influence of the pile-embedment length on the displacement accumulation. As expected, for test series 4 (c) with cyclic load magnitude of $\zeta_b = 0.2$ (instead of $\zeta_b = 0.35$), significantly smaller pile head displacements $y_{head,N=1}$ have been measured for the first load cycle. The slopes of those curves nevertheless seem not to be affected significantly and are therefore similar to that of other tests on pile-soil system 2 (grey lines) with $\zeta_b = 0.35$. In general, the results are quite consistent. Anyway, some scattering can be observed for the initial displacements $y_{head,N=1}$ resulting from the first load cycle. The scattering may be explained by some deviations of the soil relative density resulting from the sand sample preparation procedure. To eliminate the influence of slightly varying experimental boundary conditions pile head displacement accumulations $\Delta y_{head,N}$ have been calculated and normalised by the maximum pile head displacement occurring within the first load cycle ($y_{head,N=1}$). Corresponding variations of the normalised accumulations derived from the results depicted in Fig. 6(a) are provided in Fig. 6(b). For the accumulation, the differences between pile-soil system 1 and pile-soil system 2 are diminished. Anyway, different slopes of the variations for both systems can be observed. In contrast to the pile head displacement (Fig. 6(a)), the normalised pile head displacement accumulation (Fig. 6(b)) can be seen to follow a linear trend only for load cycle numbers of more than 500. Anyway, from this point ($N > 500$) the linear variation for each test confirm the general suitability of a power function to describe and extrapolate pile displacement accumulation. The constant slope of the accumulation graphs indicates an also constant accumulation factor α dependent on the pile-soil system or the pile embedment length respectively.

To determine the accumulation parameter α, all test results for cyclic load ratio $\zeta_c = 0$ and load cycle number of $N > 500$ have been fitted by a power function according to Eq. (12).

$$\frac{y_{head,N} - y_{head,N=1}}{y_{head,N=1}} = \frac{\Delta y_{head,N}}{y_{head,N=1}} = T \cdot N^{\alpha} \tag{12}$$

Table 5
Cyclic load magnitude ζ_b in dependence on pile failure criterion.

System	e/L	Manoliu et al. (1985)			$u_{failure} = 0.1$ D		$\Theta_{failure} = 4°$	
[#]	[–]	H_{ult} [N]	ζ_b [–]	H_{max} [N]	H_{ult} [N]	ζ_b [–]	H_{ult} [N]	ζ_b [–]
1	0.6	372.0	0.35	130.2	84.4	1.54	205.6	0.63
	0.8	330.0	0.35	115.5	63.6	1.82	170.6	0.68
	1.0	299.7	0.35	104.9	68.7	1.53	169.5	0.62
2	0.8	174.0	0.35	60.9	57.1	1.07	110.1	0.55
	1.0	154.0	0.35	53.9	50.3	1.07	99.4	0.54
	1.2	114.4	0.35	40.0	40.4	0.99	71.3	0.56

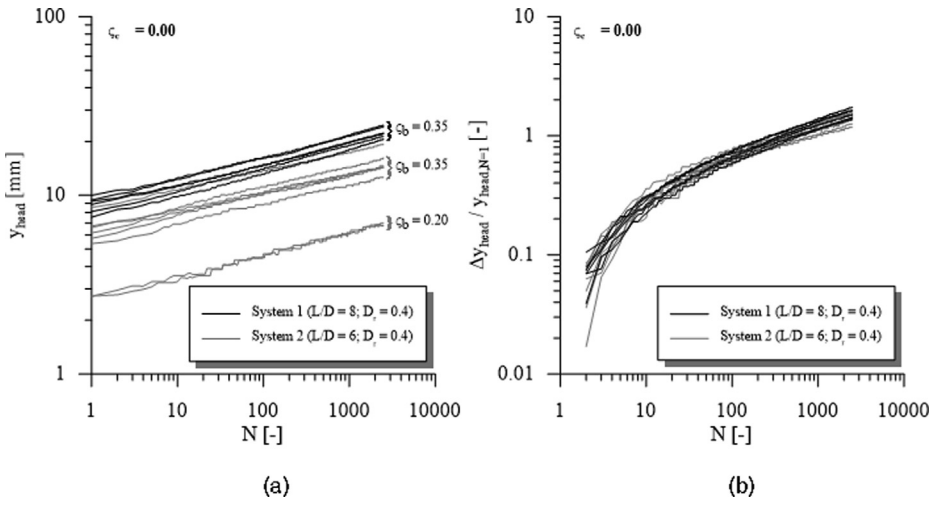

Fig. 6. (a) Pile head displacement at sand surface for cyclic tests with $\zeta_c = 0$; (b) pile head displacement accumulation for $\zeta_c = 0$.

The resulting α values for all test configurations with load magnitude of $\zeta_b = 0.35$ are plotted against L/D ratios in Fig. 7. Although some deviations exist, a clear dependency of L or L/D respectively can be observed for the exponent α, which therefore indicates a dependency of α on the pile-soil stiffness. On the other hand, a distinct influence of load eccentricity could not be identified. Therefore, the exponent α for each pile-soil system has been derived by taking mean values of the determined parameters for each L/D ratio. For pile-soil system 1 a value of $\alpha_1 = 0.24$ applies. The respective value for system 2 results to $\alpha_2 = 0.20$.

In the next step, the influence of the cyclic load ratio ζ_c on the pile head displacement accumulation shall be evaluated for each test configuration. The results of all cyclic

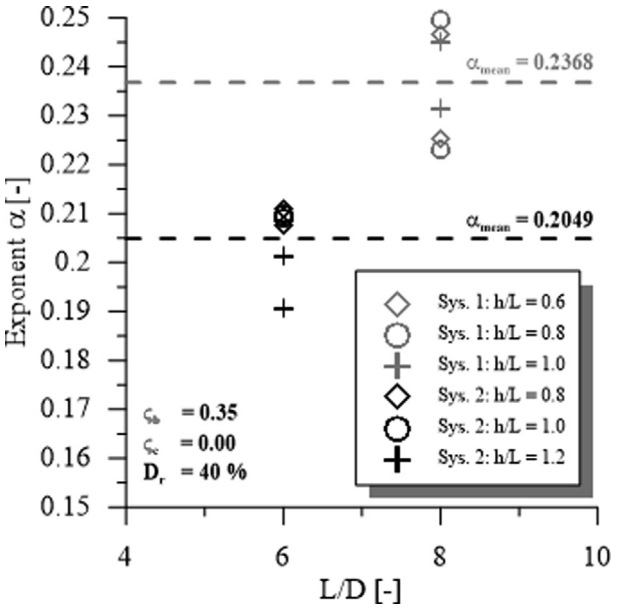

Fig. 7. Accumulation parameter α for cyclic one-way loading tests ($\zeta_c = 0$).

experiments (Test series 1–6) regarding the normalised accumulation are provided in Fig. 8. In addition to the measured accumulations, also power functions (dashed lines) for the approximation and extrapolation of the test results are depicted. These functions have been derived by fitting the results for load cycle numbers of $N > 500$ by application of Eq. (12) and the before determined accumulation parameters α_1 and α_2 for the tests on pile-soil system 1 (test series 1–3) and 2 (test series 4–6) respectively. Thereby, each function has been fitted to the results of two tests with identical boundary conditions.

From the variations depicted in Fig. 8 it emerges that highest accumulation rates, i.e. most increases in pile head displacement, apply for the first 100 load cycles. After a few hundred cycles ($100 < N < 500$) a sedative behaviour with a steady decrease in accumulation rate can be observed. Further, it can be seen that pile deflection accumulation for a given pile-soil system and load magnitude ζ_b is strongly dependent on the cyclic load ratio ζ_c. In all test series highest pile deflections and therefore accumulations could be found to result from asymmetric two-way loading at cyclic load ratio of $\zeta_c = -0.25$. On the opposite, lowest accumulations occur due to nearly symmetrical two-way loading ($\zeta_c = -0.75$) or one-way loads without complete unloading of the pile at cyclic load ratios of $\zeta_c = 0.25$.

In order to allow a comparison between the individual test series and to be able to make statements on the influence of varying test conditions (L/D, h/L, ζ_b, N) the $T_c(\zeta_c)$-function for each test series has been calculated. To derive the loading type function $T_c(\zeta_c)$ as proposed by LeBlanc et al. (2010), the parameter T from Eq. (12), which in conjunction with α describes the pile head displacement accumulation for a given pile-soil system and load eccentricity, has been normalised by the related $T(\zeta_c = 0)$ for each test. The resulting $T_c(\zeta_c)$-functions for all test series are presented in Fig. 9.

In general, it can be seen from Fig. 9 that the $T_c(\zeta_c)$-functions for both pile-soil systems and all 8 configurations

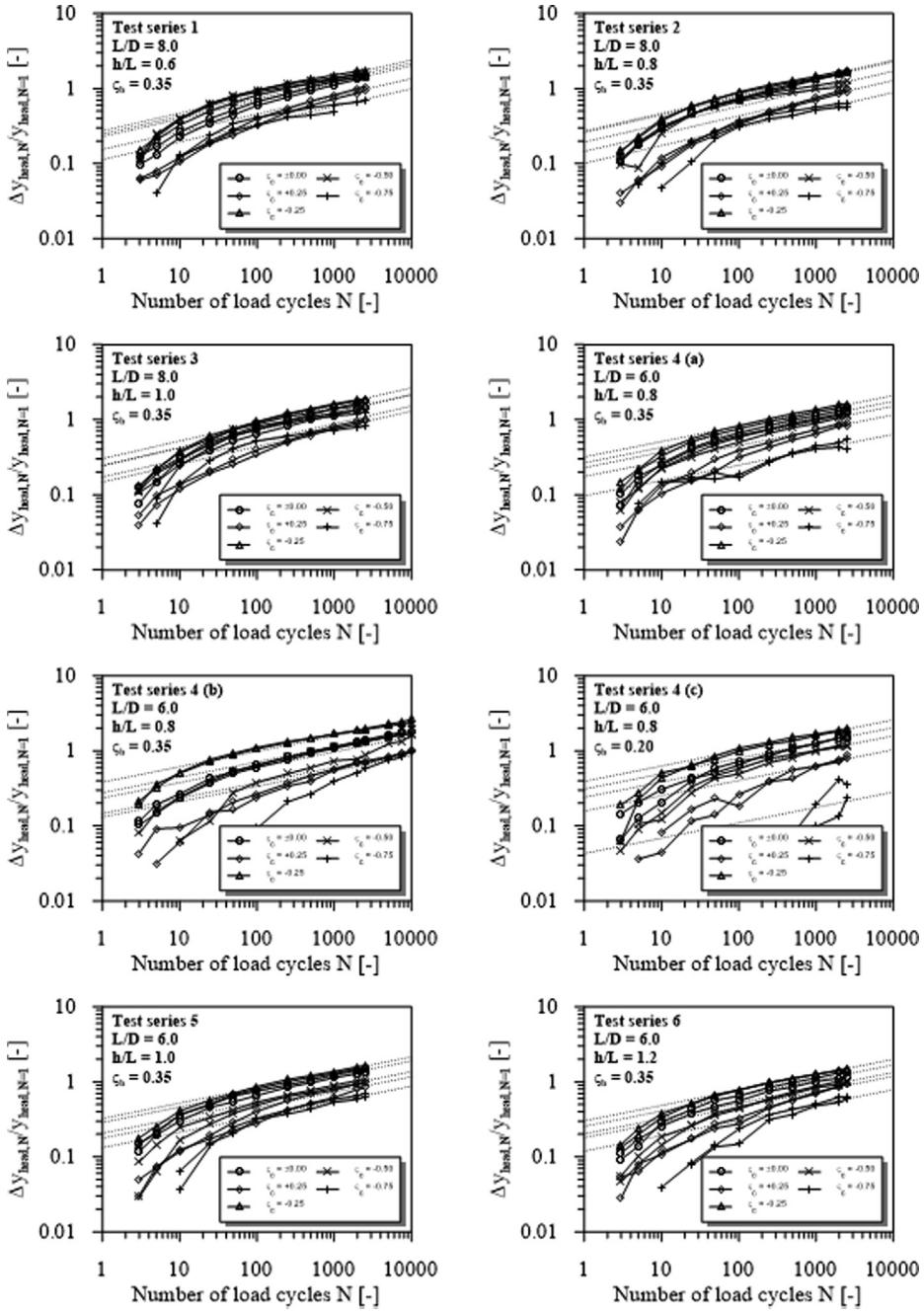

Fig. 8. Normalised pile head displacement accumulations for test series 1 to 6 and approximation functions.

are similar in shape. Highest accumulations or T_c-values respectively result from asymmetrical two-way loading with a cyclic load ratio of $\zeta_c = -0.25$ for all test series. Also the maxima of the T_c-functions do not differ significantly. Excluding test series 4 (b), which included N = 10000 load cycles and reaches a $T_{c,max} = 1.38$, the maximum values for the remaining test series are all smaller than 1.3 ranging from 1.05 to 1.27. Contrary to the observations of Albiker et al. (2017), no substantial influence of a variation in load eccentricity on the shape or maximum of the T_c-function could be identified for a given pile-soil system and relative load magnitude (see Test series 1, 2 and 3 or Test series 4 (a), 5 and 6). Comparing the results for both pile soil-systems (Fig. 9(a) and (b)) also pile embedment length seems not to change the T_c-function even though the accumulation parameter α differs for both systems. The results of test series 4 (a) and 4 (c) confirm the T_c-function of being independent from load magnitude as already proposed by LeBlanc et al. (2010). From a theoretical point of view, also the T_c-functions for test series 4 (a) with a maximum of $T_{c,max} = 1.38$ and 4 (b) showing a value of $T_{c,max} = 1.20$ should have the same shape and maximum, as the only difference between those series is the number of applied load cycles. However, since the

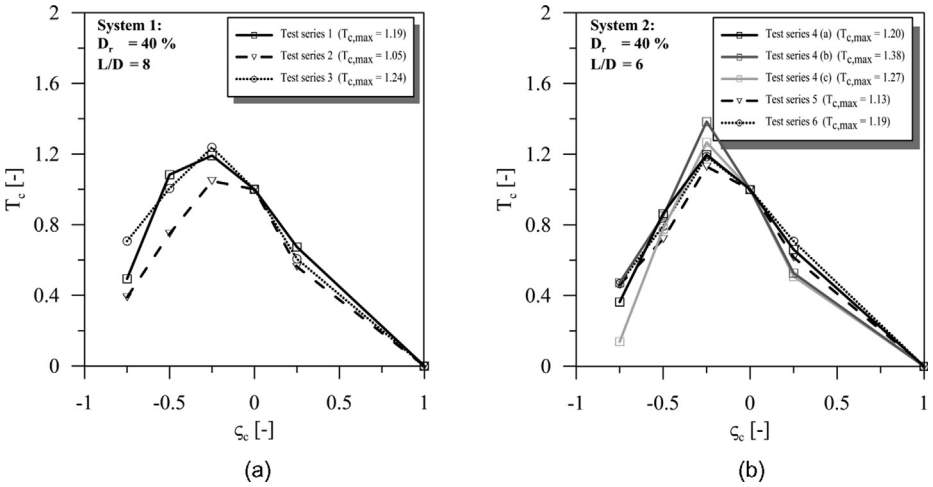

Fig. 9. $T_c(\zeta_c)$-functions for pile-soil system 1 (a) and pile-soil system 2 (b).

T_c-function is based on results of reference tests with $\zeta_c = 0$, this deviation may be explained by some irregular sand sample preparation or other experimental influences. Even slight differences in the reference tests may lead to noticeable influences on the T_c-function shape and maximum. Further repetitive tests, especially with cyclic load ratio of $\zeta_c = 0$, can help to define the T_c-function even more reliable.

4. Experimental investigation on soil rearrangement processes using particle image velocimetry

4.1. Experimental concept and set-up

To allow a better understanding of the processes leading to different pile displacement accumulations due to varying cyclic load ratios ζ_c, the model test series presented before have been supplemented by further small scale tests in which the particle image velocimetry (PIV) method has been applied to observe soil displacements around a laterally loaded pile. The PIV technique uses two consecutive digital images to correlate and calculate relative displacements between small sections of the photos, the so-called patches or subsets. Application of this method to a series of images enables the visualisation of particle paths and displacement fields throughout a series of pictures. To capture images of the pile and soil movements during either monotonic or cyclic load application, the experimental set-up depicted in Fig. 10 has been developed.

In general it consists of a narrow sand box, a rigid model pile, an actuator and a digital camera. The transparent box is made of glass with a thickness of 5 mm and inner dimensions of 1000 mm × 100 mm × 500 mm (length × width × height). The rigid model pile is a semi-circular aluminium profile with a diameter of 50 mm and an embedment length of 350 mm (L/D = 7). To ensure contact between the model pile and the transparent plane of the sand container, a second "half" pile has been arranged on the opposite side of the box. Both pile halves are slightly pressed against each other and therefore against the glass pane by three 5 mm thin threaded rods made of stainless steel (see Fig. 10). Horizontal loads have been applied with a load eccentricity of h = 50 mm using an electromechanical actuator, which is attached to both pile halves. Measurements included the applied lateral loads using a load cell installed at the actuator as well as the pile displacement at height of load application point. A digital camera (Nikon D7500, APS-C sensor) with a resolution of 5568 × 3712 pixels in combination with a 50 mm focal length lens was used to take pictures during the tests. The camera was set 80 cm in front of the box with its optical axis perpendicular to the vertical profile of the model pile. Two LED light panels were used to ensure a uniform illumination of the test set-up. To derive high contrast pictures, which is important for PIV analysis and correlation, the soil used in the tests was relatively coarse sand with grains of various colours. The model pile was also provided with a structured print on its side facing the glass pane to allow pile movements to be calculated. The sand sample was filled into the box with a shovel in layers of approximately 5 cm and around the pre-installed pile without additional compaction. The images have been processed using GeoPIV-RG, which is a free image analysis module for MATLAB and has been designed especially for geotechnical research applications (Stanier et al., 2016). The test campaign involved monotonic tests for the determination of the lateral pile capacity H_{ult} as well as two cyclic tests. Since it was the aim to identify and visualize differences in soil rearrangement processes due to different cyclic load ratios, cyclic tests have been done and evaluated for $\zeta_c = -1.0$ and $\zeta_c = -0.25$ at a load magnitude of $\zeta_b = 0.35$. Based on previous observations, it is expected that these load characteristics will lead to the greatest possible difference in behaviour under lateral cyclic loading. Due to the high computational effort involved in the evaluation of the image series of cyclic tests,

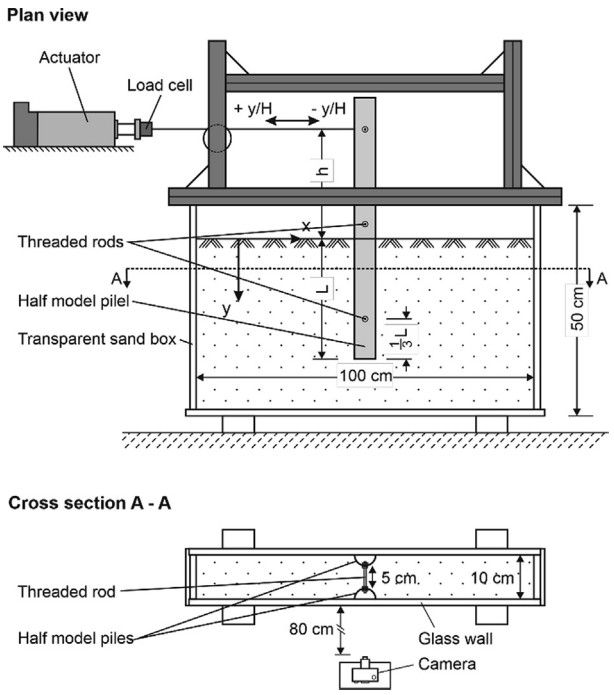

Fig. 10. Test arrangement for PIV experiments.

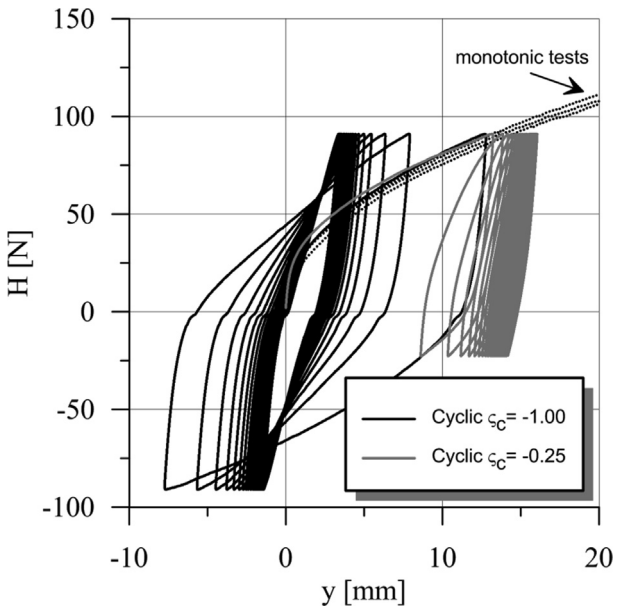

Fig. 11. Load displacement curves for monotonic and cyclic tests.

the maximum number of load cycles has been chosen to be only 25 in both cyclic experiments (resulting in about 2500 images per test and a calculation effort of approximately one week using a desktop pc). Nevertheless, this number of load cycles should be sufficient to allow clear differences due to cyclic load characteristics to be identified. In previous tests it could be observed that largest increases in pile head displacement and therefore most changes in grain structure take place within the first 100 load cycles followed by a steady decrease in accumulation rate. Therefore, most significant differences should already be visible within the first load cycles.

4.2. Evaluation of the PIV experiments

In order to determine the load-bearing capacity of the pile-soil system (D = 5 cm, L/D = 7), 3 monotonous displacement controlled tests were first carried out and evaluated. Furthermore, these tests should serve to verify the reproducibility of the sand sample preparation. Corresponding load displacement curves, where displacement y was measured 5 cm above sand surface, are depicted in Fig. 11 (dotted lines). Based on these results, the pile capacity $H_{ult} = 260$ N has been determined by application of the Manoliu et al. (1985) approach, i.e. extrapolation of the measured load displacement curves, and as the mean value of all 3 tests.

Further, the PIV-method has been applied to visualise the soil movements due to monotonic loading. From Fig. 12(a) and (b) a clear rigid body rotation of the pile with a toe kick typical for offshore monopiles could be observed. The centre of rotation can be seen to be positioned at a depth of about 275 mm, which is approximately 80% of the pile embedment length. In the direction of loading (left side), an upward directed shifting of the upper soil can be seen, whereas on the opposite site there is a significant subsidence close to the pile head (see Fig. 12(a) and (d)). Looking at the pile toe, also up (right side) and downward (left side) movements of the soil can be observed. Also in horizontal direction clearly defined zones of soil displacements can be seen. Caused by these displacements, clearly identifiable shear bands or shear zones occur on both sides of the pile. These are particularly clear from Fig. 12(c) showing the horizontal displacements only. The shearing zones are limited by regions of nearly no displacement (the transition from yellow to orange colour). While the left-sided passive soil wedge extends to a distance of about 250 mm = 5·D from the initial pile axis (at 350 mm on the x-axis), the shear band of the active soil wedge shows a significantly greater inclination and therefore a smaller extension at the soil surface of approximately 3 times the pile diameter. Large soil deformations within the shear zones indicate a large proportion of the maximum earth pressure to be already mobilised at this point.

In the next step, the cyclic test results should be analysed and compared. Corresponding load–displacement curves for both cyclic tests with symmetric ($\zeta_c = -1.0$) and asymmetric ($\zeta_c = -0.25$) two-way loading are depicted in Fig. 13. It is already apparent from the load–displacement curves that cyclic loading with $\zeta_c = -0.25$ results in an accumulation of permanent displacements, whereas for the cyclic symmetric two-way loading maximum displacements occur within the first load cycle and are followed by a negative accumulation, i.e. decreasing permanent displacements with increasing number of load cycles.

To identify the reason for this difference in behaviour, both test series have been evaluated by PIV. Fig. 13 shows

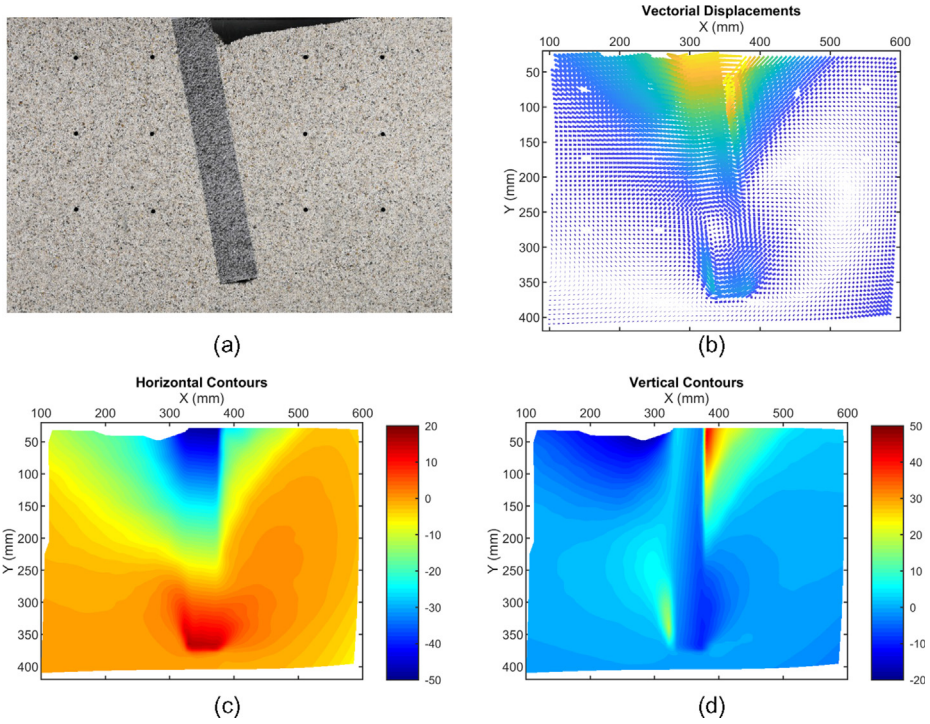

Fig. 12. PIV evaluation of a monotonic test: (a) Last image of the test series at a horizontal load of H = 179.3 N; (b) Calculated displacement vectors; (c) Contour plot horizontal displacements; (d) Contour plot vertical displacements.

the results of these calculations, where (a), (b), (c) and (d) illustrate the results for the cyclic test with an asymmetric two-way loading and Fig. 13(e), (f), (g) and (h) show the corresponding results for the cyclic test with $\zeta_c = -1.00$. All calculated results depicted in Fig. 13 show the displacements between the initial state - before horizontal loading of the pile - and the end of each test, i.e. after application of 25 load cycles. In Fig. 13(a) and (e) the last images of each test series are presented, showing the residual displacements after 25 load cycles for tests.

When comparing the results for both cyclic experiments, it emerges that in case of a symmetric two-way loading (Fig. 13, right) soil displacements also seem to be more or less symmetric. While horizontal residual displacements only reach a maximum of approximately 5 mm for this type of loading, mainly in a depth of approximately 70 mm to 150 mm and directed away from the pile (see Fig. 13(h)), the upper soil region on both sides of the pile head is dominated by very extensive vertical downward movements of up to 40 mm (see Fig. 13(g)) and a small region of horizontal displacements towards the pile. The displacements in the upper region can also clearly be seen from Fig. 13(e), where pronounced subsidence in the immediate vicinity of the pile head and on both sides can be observed, which can especially be addressed to the large downward migration of the sand while cycling. At the pile toe, also a small region of horizontal and vertical particle movements can be seen, where the soil near the pile toe is pushed into the adjacent sand leading to densification in this area and allowing some particles from above to move downward.

In case of asymmetric two-way loading vertical downward displacements almost solely take place on the right side of the pile (side of H_{min} application) and in a very limited area close to the surface. Additionally, these vertical displacements are less pronounced having a maximum of about 25 mm. In the direction of maximum cyclic load H_{max} (left side) a build-up of sand in front of the pile could be observed for $\zeta_c = -0.25$, even though this cannot be seen from Fig. 13 (left) due to the fact that the sand left the depicted region of the image defined for the PIV calculation. Looking at the horizontal displacements resulting from a cyclic load ratio of $\zeta_c = -0.25$ depicted in Fig. 13 (d), a similar behaviour as already observed in the monotonous experiments (Fig. 12(c)) can be seen. On the left side of the pile a large soil wedge is mobilised and pushed to the left in the direction of H_{max} (without noticeable vertical displacements), while the mobilised soil region on the opposite side is much smaller in horizontal direction and as already mentioned is connected with simultaneous downward movements.

Taking into account the observed differences in soil rearrangement processes from both cyclic tests described above, initial assumptions regarding the causes of a different development of pile displacement accumulation depending on the cyclic load ratio ζ_c can already be made. One reason may be a completely different development of the soil density around the pile, which of course also changes the soil stiffness. Since soil densification is always connected to a reduction in void ratio and therefore the soil volume, also stresses may be reduced in regions of compaction. During the cyclic lateral loading of the pile, and

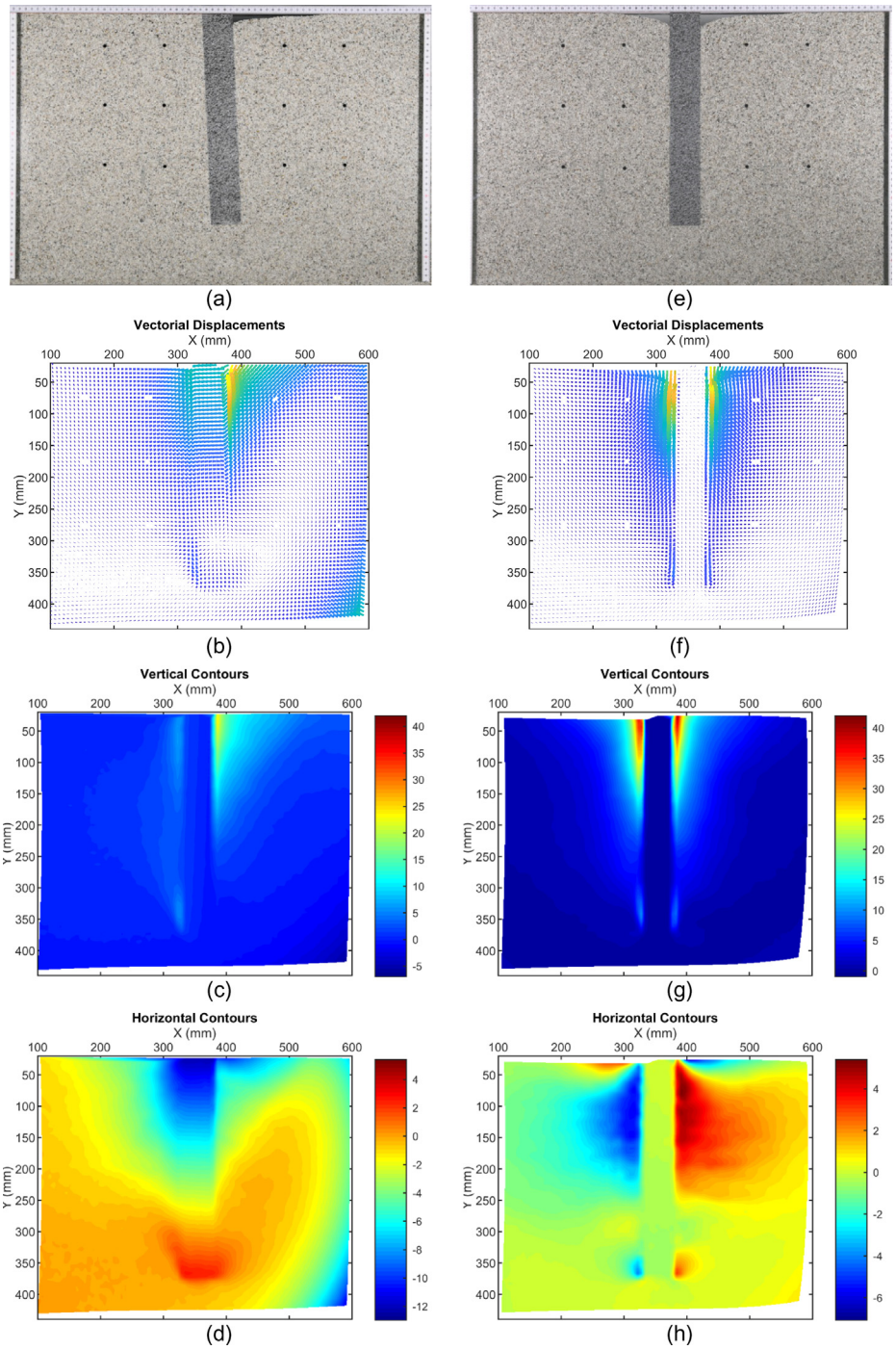

Fig. 13. PIV evaluation of cyclic tests: Permanent displacements after 25 load cycles with $\zeta_c = -0.25$ (left) and $\zeta_c = -1.0$ (right).

every time that the pile moves back after a loading peak (H_{max} or H_{min}), a stress relaxation depending on the degree of soil compaction and pile displacement amplitude takes place in the pile-soil interface. Due to this relaxation, downward migration of sand grains adjacent to the pile head and along the interface may occur. If so, the sand grains move downwards until they reach a critical depth where they again cannot move further due to increasing constraints on particle rearrangement. Within the following load cycles, the sand particles would then be pressed into the soil in horizontal direction by the advancing pile, leading to more densification until a certain limiting density is reached. From this point on the shearing behaviour of the soil dominates the pile response more than soil densification. The occurrence of this phenomenon depends on the level of stress relaxation, which in terms of a cyclic two-way loading with $\zeta_c = -1$ and a given load magnitude ζ_b of course is much higher within the first cycles than for a load with $\zeta_c = -0.25$ due to a higher pile displacement amplitude (see Fig. 11). According to these observations,

a different development of relative soil density and therefore load–displacement response under different loading types can be explained. Most densification can be seen to result from symmetrical two-way loading (or loading with higher displacement amplitude), leading to a reduction or as in this case even a negative pile displacement accumulation. The phenomenon that loads with negative cyclic load ratios close to $\zeta_c = 0$ (e.g. $\zeta_c = -0.25$) result in higher displacement accumulations compared to a cyclic one-way loading ($\zeta_c = 0$) cannot be explained by the mechanisms described above. This may be due to another mechanism leading to the least possible compaction for this type of loading, which is not yet evident from the results presented here. Further tests with a cyclic load ratio of $\zeta_c = 0$ are necessary to explain this behaviour.

5. Discussion

The results of the experimental study show that a power function as introduced in Eq. (12) provides a reasonable representation of the pile displacement accumulations measured in the cyclic tests for more than 100 load cycles. The parameters of the power function could be shown to depend on the properties of the pile-soil system and load characteristics. While the factor T of the power function is mainly influenced by the load characteristics (ζ_b and ζ_c), the results show the accumulation parameter α to depend on the pile embedment length. Therefore, the method proposed by LeBlanc et al. (2010) (see Eq. (8) and Fig. 1) seems to provide a simple and pragmatic approach to consider the different dependencies and to obtain an estimation of the expected accumulations for a given number of load cycles. A difficulty results from the reliable definition of the function parameters T_b, T_c and α. As it can be seen from the presented literature review, several experimental studies on the displacement or rotation accumulation of laterally loaded rigid monopiles have been conducted and multiple different parameters have been reported.

For the 1 g tests on almost rigid pile-soil systems conducted in this experimental study the accumulation coefficient α was found to moderately increase with pile embedment length or decrease with relative pile-soil stiffness, respectively. In case of pile-soil system 1 with a normalised embedment length of L/D = 8 an accumulation parameter of $\alpha = 0.24$ has been determined. The corresponding value for pile-soil system 2 (L/D = 6) reduced to $\alpha = 0.20$. For both pile soil-systems the α-value was not affected by a variation of load eccentricity h, which seems to be reasonable due to the definition of the applied maximum cyclic loads by the relative load magnitude ζ_b for each configuration. In addition, it could be shown that also cyclic load magnitude has no significant influence on the accumulation parameter α. Compared to literature values, the determined accumulation coefficients seem to be in a plausible range although they are not equal. While LeBlanc et al. (2010) propose a value of $\alpha = 0.31$ for a monopile with L/D = 4.5 in coarse sand, Albiker et al. (2017) found an accumulation coefficient of $\alpha = 0.23$ to fit their results best (L/D = 5.8, fine to medium sand). For the accumulation of permanent rotations of a laterally loaded caisson foundation values of $\alpha = 0.39$ in fine silty sand (Zhu et al., 2013) and $\alpha = 0.18$ in fine sand (Foglia, 2014) have been reported. Obviously, α is not only dependent on pile embedment length or L/D-ratio but may also be influenced by other factors (e.g. grain size distribution). Additional tests are required to identify the parameters affecting the accumulation coefficient α. Moreover, it has to be kept in mind that according to Richards et al. (2020) α-values are stress dependent and those obtained by scaled 1 g model tests may be reduced, when applied to true scale monopiles (see chapter 3: scaling considerations).

Further, the influence of cyclic load ratio ζ_c has been investigated and T_c-functions for all 8 test configurations have been derived. Independent of the underlying pile embedment length or load eccentricity, a maximum pile head displacement accumulation could be found to result from an asymmetric two-way loading with $\zeta_c = -0.25$. Excluding test series 4 (b) with an applied load cycle number of N = 10000, determined maximum T_c-values range from 1.05 to 1.27 (test series 4 (b): $T_{c,max} = 1.38$). Similar to LeBlanc et al. (2010) no significant influence of the load magnitude ζ_b on the shape of the T_c-function or its maximum could be identified (see test series 4 (a) and 4 (c)). An influence of the load eccentricity on $T_{c,max}$, as supposed by Albiker et al. (2017), could not be verified. Anyway, a comparison of the determined T_c-functions with those found in literature approves the general shape of the T_c-function for rigid piles in sand that reaches its maximum value for an asymmetric two-way loading. Typical literature values for the most critical cyclic load ratio $\zeta_c(T_{c,max})$ leading to maximum accumulations are in the range of $\zeta_c = -0.33$ and $\zeta_c = -0.6$ (see Table 5), which is close to the determined value of $\zeta_c = -0.25$. Minor differences in $\zeta_c(T_{c,max})$ could result from different soil types, among other things. However, comparing the maximum values of the T_c-functions depicted in Table 6 and those derived in the tests reported in this study, it emerges that significant differences exist. While LeBlanc et al. (2010) or Arshad and O'Kelly (2017) found maximum T_c-values of approximately 4 or even higher for related cyclic load ratios of $\zeta_c = -0.6$ and $\zeta_c = -0.5$, Klinkvort and Hededal (2013) determined highest accumulations due to a cyclic loading with $\zeta_c = -0.4$, where $T_{c,max}$ was only slightly greater than 1. With $T_{c,max}$-values of 1.05 to 1.38, the results of this study can be placed rather in the lower range of the previously mentioned results. The reason for the very large range of $T_{c,max}$ is most likely due to the fact that the T_c-function is very sensitive to the way the experimental results are approximated and evaluated, respectively. Furthermore, even smallest errors in the test procedure (e.g. slight deviations from the targeted relative soil density, faulty application of cyclic

Table 6
$T_{c,max}$-values and related ζ_c-ratios reported by various authors.

Author	D [mm]	L/D [–]	e/L [–]	D_r [%]	$T_{c,max}$ [–]	$\zeta_c(T_{c,max})$ [–]
LeBlanc et al. (2010)	80	4.5	1.19	4/38	≈4	≈−0.6
Klinkvort and Hededal (2013)	28	6	2.5	90	Slightly	−0.4
	40	6	2.5	90	greater 1	−0.4
Arshad and O'Kelly (2017)	53	6.7	0.25	70–74	1.25–4.50	−0.5
Albiker et al. (2017)	60	5.8	0.36	44	1.35	−0.33
	60	5.8	0.71	44	1.72	−0.33
This study	50	8	0.6	40	1.19	−0.25
	50	8	0.8	40	1.05	−0.25
	50	8	1.0	40	1.24	−0.25
	50	6	0.8	40	1.20	−0.25
	50	6	0.8	40	1.38	−0.25
	50	6	0.8	40	1.27	−0.25
	50	6	1.0	40	1.13	−0.25
	50	6	1.2	40	1.19	−0.25

loads, etc.) lead to significant changes in the deformation accumulation and thus in the T_c-function or its maximum. For this reason, the study presented here involved repetitive tests to prove repeatability and to minimise the influence of unintended test scattering. Due to the large number of tests, the derived T_c-functions can be considered relatively reliable. Nevertheless, it is possible that also other boundary conditions that have not been investigated here influence the shape and maximum of the T_c-function. More experiments and in particular large scale field tests or measurements on existing monopile foundations are desirable for further clarification.

6. Conclusions

This paper has presented results of an extensive series of small scale 1 g model tests on laterally loaded piles in sand. Additionally, experiments involving the visualisation of resulting soil displacements by particle image velocimetry have been described. All the above tests have added new insights into the factors controlling the cyclic displacement accumulation of a laterally loaded pile. The following main conclusions can be drawn:

- Cyclic test results confirm the suitability of a power function (Eq. (12)) to approximate and extrapolate cyclic pile displacement accumulation for load cycle numbers of $N > 100$. As proposed by LeBlanc et al. (2010), the function parameters are dependent on cyclic load characteristics, pile dimensions and soil conditions (see Eq. (3)).
- The accumulation coefficient α varies slightly for different systems, since it seems to be affected by both pile geometry (L/D) and soil type.
- Highest accumulation rate occurs for asymmetric two-way loading. Regarding the maximum of the T_c-function, preceding studies showed a rather large bandwidth. The tests conducted here revealed $T_{c,max}$-values only slightly greater than 1 (around 1.2) being independent of load magnitude. For a given load magnitude, also load eccentricity has no significant influence on the shape or maximum of the T_c-function.
- Observation of deformation patterns in the soil around the monopile by PIV indicate that the reason for greater accumulation rates at asymmetric two-way loading is that minimum net soil compaction occurs around the pile. However, more such tests are necessary to prove this assumption.

Acknowledgement

This study was carried out in the scope of the research project "Accumulation of lateral displacements of piles under general cyclic one- and two-way loading" (project no. 393683178) funded by German Research Foundation (DFG). The authors sincerely acknowledge DFG support.

References

Albiker, J., 2016. Untersuchung zum Tragverhalten zyklisch lateral belasteter Pfähle in nichtbindigen Böden. Ph.D. Thesis. Leibniz Universität Hannover, Germany.

Albiker, J., Achmus, M., Frick, D., Flindt, F., 2017. 1g model tests on the displacement accumulation of piles under general cyclic one- and two-way loading. Geotech. Test. J., ASTM 40 (2), 173–184.

API, 2014. Recommended practice 2GEO - Geotechnical and Foundation Design Considerations. American Petroleum Institute, Washington, RP2A-WSD, 22nd edition.

Arshad, M., O'Kelly, B.C., 2017. Model studies on monopile behaviour under long-term repeated lateral loading. Am. Soc. Civil Eng. (ASCE) Int. J. Geomech. 17 (1).

Byrne, B.W., Burd, H., Mcadam, R., Houlsby, G.T., 2017. PISA: New design methods for offshore wind turbine monopiles. Proceedings of the 8th International Conference Offshore Site Investigation and Geotechnics (OSIG), pp. 142–161.

Byrne, B.W., Burd, H.J., Zdravkovic, L., Abadie, C.N., Houlsby, G.T., Jardine, R.J., Martin, C.M., McAdam, R.A., Pacheco Andrade, M., Pedro, A.M.G., Potts, D.M., Taborda, D.M.G., 2019. PISA design methods for offshore wind turbine monopiles. Offshore Technol. Conf. https://doi.org/10.4043/29373-ms.

DNV GL, 2018. DNVGL-ST-0126 - Support structures for wind turbines. Det Norske Veritas, Oslo.
Foglia, A., 2014. Bucket foundations under lateral cyclic loading. Ph.D. thesis. Aalborg University, Denmark.
Hoadley, P., Barton, Y., Parry, R., 1981. Cyclic lateral load on model pile in a centrifuge. Proceeding of the International Conference on Soil Mechanics and Foundation Engineering, pp. 621–625.
Jalbi, S., Arany, L., Salem, A., Cui, L., Bhattacharya, S., 2019. A method to predict the cyclic loading profiles (one-way and two-way) for monopile supported offshore wind turbines. Mar. Struct. 63, 65–83.
Kallehave, D., LeBlanc Thilsted, C., Liingaard, M.A., 2012. Modification of the API p-y formulation of initial stiffness of sand. Proceedings of the 7th International Conference Offshore Site Investigation and Geotechnics (OSIG), pp. 465–472.
Klinkvort, R.T., 2012. Centrifuge Modeling of drained lateral pile-soil response. Ph.D. thesis. Technical University of Denmark, Lyngby, Denmark.
Klinkvort, R.T., Hededal, O., 2013. Lateral response of monopile supporting an offshore wind turbine. Geotech. Eng. 166 (GE2), 147–158.
LeBlanc, C., Houlsby, G.T., Byrne, B.W., 2010. Response of stiff piles in sand to long-term cyclic lateral loading. Géotechnique, ICE 60 (2), 79–90.
Li, W., Igoe, D., Gavin, K., 2015. Field tests to investigate the cyclic response of monopiles in sand. Proc. Inst. Civil Eng. – Geotech. Eng., ICE 168 (5), 407–421.
Lin, S., Liao, J., 1999. Permanent strains of piles in sand due to cyclic lateral loads. J. Geotech. Geoenviron. Eng. 125 (9), 798–782.
Long, J., Vanneste, G., 1994. Effects of cyclic lateral loads on piles in sand. J. Geotech. Eng. 120 (1), 225–244.
Manoliu, I., Dimitriu, D.V., Radulescu, N., Dobrescu, G., 1985. Load-deformation characteristics of drilled piers. In: Proceedings of the 11th International Conference on Soil Mechanics and Foundation Engineering, vol. 3, pp. 1553–1558.
Murchison, J., O'Neill, M., 1984. Evaluation of p-y- relationships in cohesionless soils. Proc. Anal. Des. Pile Foundat., 174–191
Peralta, P., Achmus, M., 2010. An experimental investigation of piles in sand subjected to lateral cyclic loads. Proceedings of the 7th International Conference on Physical Modelling in Geotechnics, pp. 985–990.
Poulos, H.G., Hull, T., 1989. The role of analytical geomechanics in foundation engineering. Foundat. Eng.: Curr. Principles Practice, ASCE, 1578–1606.
Reese, L.C., Cox, W.R., Koop, F.D., 1974. Analysis of laterally loaded piles in sand. Proceedings of the Offshore Technology Conference, pp. 473–483.
Richards, I.A., Bransby, M.F., Byrne, B.W., Gaudin, C., Houlsby, G.T., 2020. The effect of stress-level on the response of a model monopile to cyclic lateral loading in sand. J. Geotech. Geoenviron. Eng., accepted manuscript.
Rosquoët, F., Thorel, L., Garnier, J., Canepa, Y., 2007. Lateral cyclic loading of sand-installed piles. Soils Found. 47 (5), 821–832.
Sørensen, S.P.H., 2012. Soil-structure interaction for non-slender, large diameter offshore monopiles. Ph.D. Thesis, Aalborg University, Denmark, Department of Civil Engineering.
Stanier, S.A., Blaber, J., Take, W.A., White, D.J., 2016. Improved image-based deformation measurement for geotechnical applications. Can. Geotech. J. 53 (5), 727–739.
Thieken, K., Achmus, M., Lemke, K., 2015. A new static p-y approach for piles with arbitrary dimensions in sand. Geotechnik 38 (4), 267–288.
Truong, P., Lehane, B.M., 2015. Experimental trends to lateral cyclic tests of piles in sand. In: Proceedings of the 3rd International Symposium on Frontiers in Offshore Geotechnics, Oslo/Norway, vol. I, pp. 747–752.
Truong, P., Lehane, B.M., Zania, V., Klinkvort, R.T., 2019. Empirical approach based on centrifuge testing for cyclic deformations of laterally loaded piles in sand. Géotechnique 69 (2), 133–145.
Walsh, C., 2019. Offshore Wind in Europe – Key Trends and statistics 2018. Wind Europe, Brussels.
Zhu, B., Byrne, B.W., Houlsby, G.T., 2013. Long-term lateral cyclic response of suction caisson foundations in sand. J. Geotech. Geoenviron. Eng., ASCE 139 (1), 73–83.